Hydrothermal Synthesis and Characterisation of Two Novel Large-Pore Framework Vanadium Silicates

Paula Brandão,[a] Anabela Valente,[a] Andreas Philippou,[b] Artur Ferreira,[c] Michael W. Anderson,[b] and João Rocha*[a]

Keywords: Microporous materials / Silicates / Vanadium / Catalysis / Hydrothermal synthesis

Two new large-pore sodium vanadium silicates, denoted AM-15 and AM-17 (Aveiro-Manchester, structures number 15 and 17) with framework composition $Na_6Si_{14}V_4O_{39}$ and $Na_4CaSi_{10}V_2O_{27}$, respectively, are reported. Electron paramagnetic resonance (EPR), Fourier transform infrared (FTIR) and diffuse reflectance ultraviolet-visible (DR UV/Vis) spectroscopy reveal that as-prepared AM-15 contains both V^{IV} and V^{V} in a square pyramidal and tetrahedral coordination, respectively, while AM-17 contains predominantly octahedral V^{IV}. The thermal stability of AM-15 in air is modest (ca. 380 °C), while AM-17 is stable up to 450 °C. The acid-base and redox properties of AM-17 have been assessed by the conversion of isopropanol and ethanol oxidation, respectively.

Introduction

Microporous vanadium silicates are a new class of materials with potential for applications as selective heterogeneous catalysts for acid-catalysed and oxidation reactions.[1−3] In such systems, catalyst deactivation is a major issue, associated with reduced thermal stability and leaching phenomena.[4] As a result, much research has been carried out in order to prepare vanadium silicates with improved catalytic behaviour.[5−14]

In 1997 we reported the first example of a large-pore vanadium silicate containing stoichiometric amounts of hexacoordinate vanadium (Si/V = 5).[15] This material, dubbed AM-6, is a structural analogue of titanium silicate ETS-10, where titanium has been fully replaced by vanadium. ETS-10 has a framework consisting of "TiO_2" rods, which run in two orthogonal directions and are surrounded by tetrahedral silicate units. The pore structure consists of twelve-, seven-, five- and three-membered rings and has a three-dimensional channel system whose minimum diameter is defined by twelve-membered ring apertures.[16] Jacobson and co-workers reported two novel small-pore vanadium silicates $K_2(VO)(Si_4O_{10})\cdot H_2O$ (VSH-1) and $Cs_2(VO)(Si_6O_{14})\cdot 3H_2O$ (VSH-2), whose structures are closely related to the structures of cavansite and pentagonite.[17] Cavansite and pentagonite, dimorphs of the mineral $Ca(VO)(Si_4O_{10})\cdot 4H_2O$, are small-pore materials containing V^{IV} in a square-pyramidal coordination.[18,19] The framework of cavansite is formed by silicate layers of four- and eight-membered rings of tetrahedra connected vertically by V^{IV} cations. Calcium cations and water molecules reside in the channels formed by the eight-membered rings and between the SiO_2 layers. Cavansite has channels running parallel to the *c* direction with a free diameter of only 3.3 Å in the hydrated state. Recently, the same authors reported on a series of novel vanadium silicates with open-framework and microporous structures with general formula $A_r[(VO)_s(Si_2O_5)_p(SiO_2)_q]\cdot tH_2O$, where A is Na, K, Rb, Cs, or a combination of these metals.[20] Two other large-pore vanadium silicates, AM-13 and AM-14 with Si/V molar ratios of 4 and 10, respectively, have also been reported.[21] In the as-prepared samples, both V^{IV} and V^{V} occur simultaneously in different coordination environments. Like AM-6, AM-14 contains essentially hexacoordinate V^{IV}, while in AM-13 V^{IV} may be in a square-pyramidal coordination. The preparation of these two materials depends strongly on variables such as gel pH, cations present, time and temperature.[22] AM-13 requires a pH between 10.6 and 11.0 whereas AM-14 is obtained in the pH range 10.3−10.5. The AM-13 gel contains 60% Na and 40% Ca, whereas AM-14 crystallises in the presence of Na cations. Here we wish to report the synthesis and characterisation of two novel large-pore vanadium silicates, AM-15 and AM-17.

[a] Department of Chemistry, University of Aveiro, CICECO, 3810-193 Aveiro, Portugal
Fax: (internat.) + 351-34/370-084
E-mail: ROCHA@DQ.UA.PT
[b] Department of Chemistry, UMIST, P. O. Box 88, Manchester M60 1QD, UK
[c] ESTGA, University of Aveiro, CICECO, 3810-193 Aveiro, Portugal

Results and Discussion

Powder XRD

The powder XRD patterns of AM-15 and AM-17 are shown in Figure 1 with the corresponding d-spacings and intensities listed in Table 1 and 2, respectively. The AM-15 cell is monoclinic with $a = 29.612$, $b = 17.892$, $c = 11.400$ Å, $\beta = 97.39°$ (volume 5990 Å^3). The most probable space group is $P2_1/n$ (no.14). The AM-17 cell is orthorhombic with $a = 37.712$, $b = 26.973$, $c = 16.456$ Å, (volume 16740 Å^3). The most probable space group is *Pba*2 (no. 32).

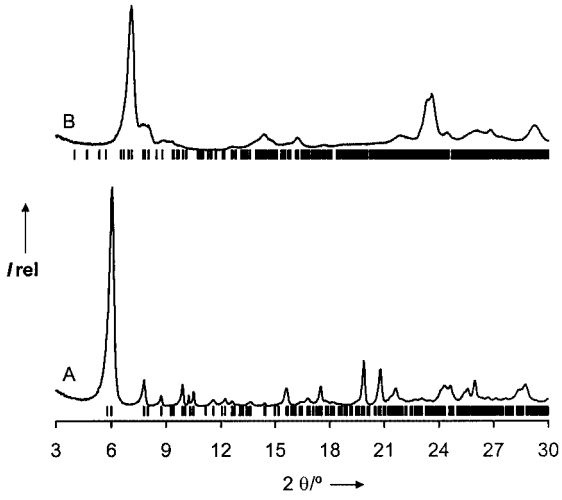

Figure 1. Powder XRD patterns of: A) AM-15 and B) AM-17; the tick marks depict Bragg reflections

Table 1. Powder XRD data of AM-15

d (Å)	I/I_0	d (Å)	I/I_0
14.568	100	4.273	17
11.332	12	4.106	7
10.110	5	3.917	1
8.923	10	3.855	2
8.410	7	3.663	7
7.643	3	3.612	7
7.224	3	3.478	5
7.011	2	3.429	10
6.503	2	3.340	1
6.144	1	3.283	1
5.672	8	3.226	1
5.399	1	3.143	5
5.286	3	3.108	8
5.064	9	2.972	2
4.890	1	2.929	4
4.465	22	2.899	5

SEM and EDAX

SEM images of the AM-15 samples (Figure 2) reveal that the crystals consist of thin plates with a particle size of ca. 5 μm. EDAX analysis of different AM-15 crystals shows a similar molar composition: Si/V = 3.7, Na/V = 1.5. No other phases rich in silicon or vanadium were detected. Assuming that all vanadium is present as V^{IV} (which is probably not entirely correct, see below) the ideal formula of dehydrated AM-15 is $Na_6Si_{14}V_4O_{39}$. AM-17 crystals consist of plates with a size of ca. 1−2 μm, with the following molar ratios: Si/V = 4.4, Na/Ca = 2.9, Na/V = 1.0. The ideal formula of AM-17 is $Na_6Ca_2Si_{24}V_6O_{65}$, where all vanadium is assumed to be present as V^{IV}.

Table 2. Powder XRD data of AM-17

d (Å)	I/I_0	d (Å)	I/I_0
21.674	<1	5.006	2
16.325	<1	4.729	2
12.394	100	4.079	8
11.397	17	4.052	8
10.974	16	3.800	34
9.987	5	3.765	38
9.448	5	3.637	9
9.123	3	3.521	5
7.037	2	3.503	7
6.864	2	3.433	10
6.499	3	3.405	11
6.343	6	3.321	11
6.165	11	3.134	4
5.991	6	3.066	13
5.638	4	3.049	14
5.459	7	3.031	10

Thermal Analysis

The thermal stability of AM-15 and AM-17 was investigated using TGA/DSC in air, and variable temperature (25−650 °C) in-situ powder XRD in air and in vacuo. The AM-15 and AM-17 total mass loss between 30 and 600 °C is ca. 12.0% and 9.8%, respectively. DSC exhibits exothermic peaks centred at 380 °C (AM-15) and 450 °C (AM-17) probably due to the collapse of the crystalline structure (Figure 3). When calcined in vacuo, both materials retain their structural integrity up to about 600 °C (not shown). Upon calcination in air at temperatures of ca. 400 °C the structure of AM-15 collapses, while AM-17 is stable until ca. 450 °C (Figure 4).

Adsorption Measurements

Nitrogen adsorption isotherms are of type I, with a slight upward distortion (Figure 5), suggesting that microporosity (pore width < 2 nm, according to IUPAC) is associated with significant external surface area. These vanadium silicates have similar specific surface areas (330−380 m^2/g) and micropore volumes (0.1−0.13 cm^3/g; Table 3). A narrow pore-size distribution with median pore width of 8 and 7.3 Å is obtained for AM-15 and AM-17, respectively. Both materials adsorb benzene, *m*-xylene and mesitylene and the sorption capacities (taken at $p/p_0 \approx 0.4$) decrease with increasing size of the diffusing molecule (molecular dimension in brackets): benzene (6.8 Å) > *m*-xylene (7.4 Å) > mesitylene (8.4 Å; Table 4). The above results suggest that AM-15 and AM-17 have large accessible pores with a width of 7−8 Å.

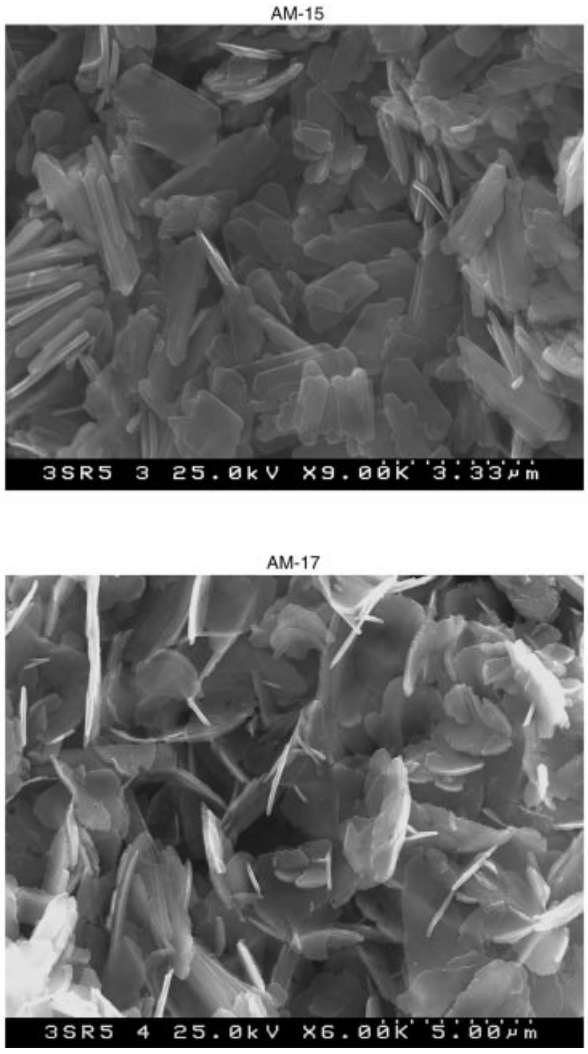

Figure 2. SEM images of AM-15 and AM-17

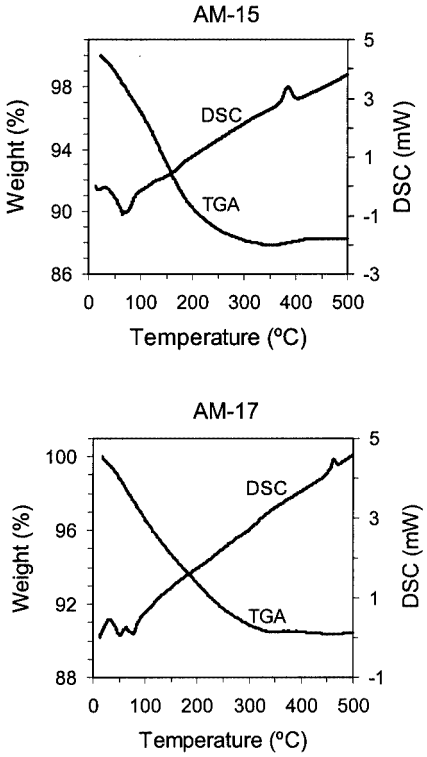

Figure 3. TGA and DSC curves of AM-15 and AM-17, recorded in air

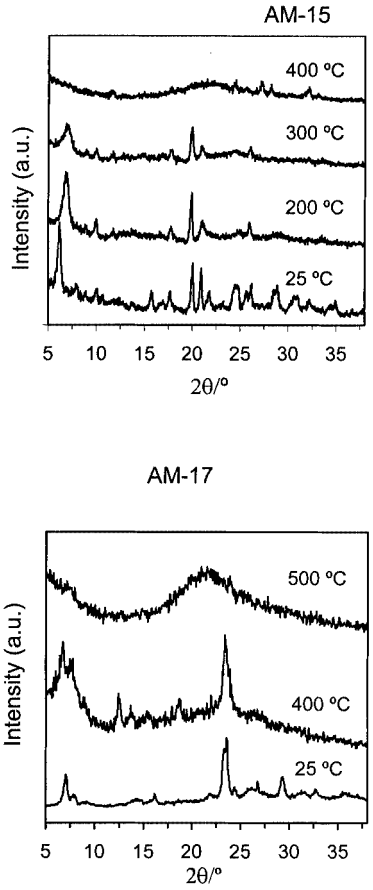

Figure 4. Powder XRD patterns of AM-15 and AM-17, recorded in situ at different temperatures in air

Electron Paramagnetic Resonance

The oxidation state of vanadium atoms in as-synthesised AM-15 and AM-17 was studied by EPR spectroscopy at room temperature. The spectra of AM-15 and AM-17 display a broad signal centred at $g = 2.357$ and 2.415, respectively (Figure 6). No hyperfine structure is observed, indicating the presence of (nonisolated) V^{IV} dipolar-coupled to other V^{IV} ions.

Fourier Transform Infrared Spectroscopy

FTIR spectra of AM-15, AM-17 and, for comparison, AM-6 and crystalline V_2O_5 (Aldrich) are shown in Figure 7. Since the characteristic FTIR bands at $\tilde{\nu} = 838$ and 605 cm^{-1} are not observed, the presence of crystalline V_2O_5 in AM-15 and AM-17 is ruled out. The band at $\tilde{\nu} = 872$ cm^{-1} in the spectrum of AM-6 is ascribed to V^{IV} in an octahedral coordination. The IR absorption spectrum of AM-17 shows a small band at $\tilde{\nu} = 887$ cm^{-1} which, by comparison with

Table 3. Texture parameters of AM-15 and AM-17

Sample	S_{Lang}[a] (m^2/g)	TPV [b] (cm^3/g)	$V_{micropore}$ [c] (cm^3/g)	Pore size [d] (Å)
AM-15	375	0.17	0.13	8.0
AM-17	337	0.16	0.11	7.3

[a] Langmuir specific surface area. [b] Total pore volume. [c] Micropore volume derived from t-plot. [d] Median pore diameter derived from DFT calculations.

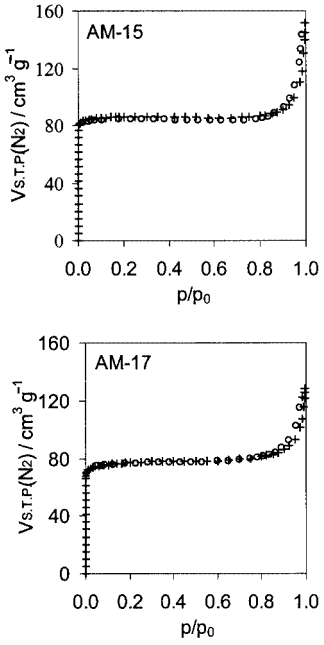

Figure 5. Nitrogen adsorption (+) and desorption (O) isotherms of AM-15 and AM-17

Table 4. Adsorption of hydrocarbons on AM-15 and AM-17 at 298 K

Sample	Benzene	*m*-Xylene ($\mu mol \cdot g_{solid}^{-1}$) [a]	Mesitylene
AM-15	740	430	248
AM-17	910	526	304

[a] Uptake at $p/p_0 \approx 0.4$.

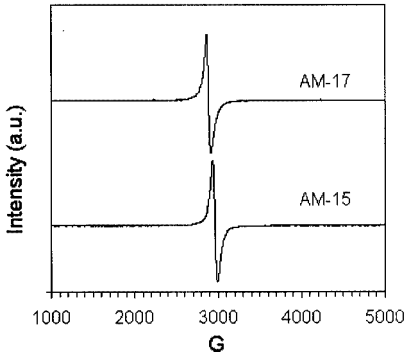

Figure 6. Room temperature EPR spectra of AM-15 and AM-17

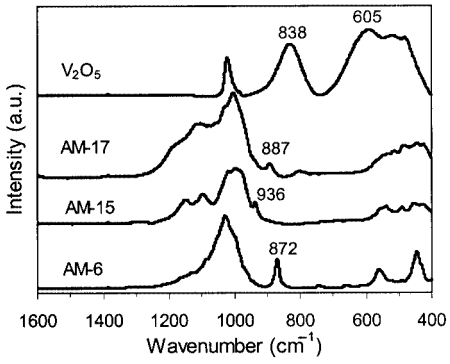

Figure 7. FTIR absorption spectra of AM-15, AM-17, AM-6 and V_2O_5

AM-6, is assigned to hexacoordinate V^{IV}. The AM-15 band at $\tilde{\nu} = 936\ cm^{-1}$ indicates the presence of V=O bonds, which usually give bands in the region $\tilde{\nu} = 900-1000\ cm^{-1}$.[23] No band is observed in the range of octahedral V^{IV}.

Diffuse-Reflectance UV/Visible Spectroscopy

Additional structural information on vanadium coordination may be obtained by DR UV/Vis spectroscopy. AM-6 is used as a DR UV/Vis reference compound, since it contains hexacoordinate V^{IV}. All samples exhibit broad bands at about 600, 435, and 220−270 nm (Figure 8). Charge transfer (CT) associated with O to V^{IV} electron transfer occurs in the range 220−270 nm.[10,24] The bands at 600 and 435 nm are assigned to V^{IV} d-d transitions and are responsible for the green colour of the solids. These observations suggest that both vanadium silicates contain V^{IV}. However, AM-15 gives a band at 340 nm, which is absent from the AM-6 and AM-17 spectra. In general, the spectra of materials containing V^{V} ions exhibit CT absorption bands in the region 280−340 nm.[9,25] Therefore, the AM-15 UV band observed in this region may be ascribed to the presence of tetrahedral V^{V}. Combining the DR UV/Vis and FTIR evidence, we propose that in AM-15 V^{IV} and V^{V} may be in a square pyramidal and tetrahedral coordination, respectively, while AM-17 contains essentially hexacoordinate V^{IV}.

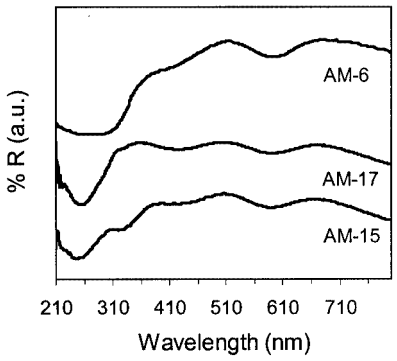

Figure 8. Diffuse reflectance UV/Vis spectra of AM-6, AM-15 and AM-17

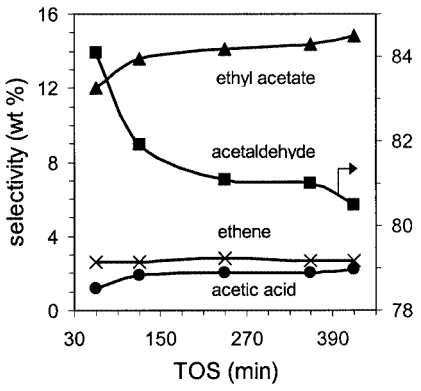

Figure 9. Effect of TOS on the products distribution of ethanol oxidation (T = 300 °C; WHSV = 0.4 h^{-1}), over AM-17

Catalytic Tests

Given the modest thermal stability of AM-15 the catalytic reactions in the gas phase were carried out over AM-17.

Isopropanol Conversion

A preliminary characterisation of the acid-base properties of AM-17 was performed by means of 2-propanol conversion, a probe reaction which is tailored for both acidity and basicity.[26] AM-17 yields mainly acetone, resulting from base-catalysed dehydrogenation of 2-propanol, whereas propene, formed by acid-catalysed dehydration, was produced in smaller amounts (Table 5). These results point to the basic character of AM-17.

Ethanol Oxidation

The oxidation activity of AM-17 was studied using the oxidation of ethanol with air as a model reaction.[27] The catalytic results obtained at 300 °C are shown in Table 5. AM-17 yields mainly acetaldehyde (84.1% selectivity at 23.7% conversion) and ethyl acetate (12% selectivity), along with minor amounts of ethene and acetic acid. Acetaldehyde is formed in the dehydrogenation process. As seen in Figure 9, long times on stream (TOS) favour the formation of ethyl acetate at the expense of acetaldehyde. The consecutive reaction of acetaldehyde with ethanol and oxygen produces ethyl acetate.[28,29] AM-17 possesses little dehydration activity in this process, evidenced by the formation of minor amounts of ethene (2.3% selectivity). After the catalytic tests, AM-17 was characterised by powder XRD, and the results show 21% crystallinity loss. The above results indicate that AM-17 is a basic solid with potential in redox catalysis.

Table 5. Conversion and product selectivity (wt %) of 2-propanol.[a] and ethanol oxidation[b] over AM-17

	Isopropanol	Ethanol
Conversion	31.2	23.7
Acetone	73.8	–
Propene	26.2	–
Acetaldehyde	–	84.1
Ethyl acetate	–	12.1
Ethene	–	2.6
Acetic acid	–	1.2

[a] $T_{reaction}$ = 350 °C; TOS = 60 min; WHSV = 2 h^{-1}; carrier gas: argon. [b] $T_{reaction}$ = 300 °C; TOS = 60 min; WHSV = 0.4 h^{-1}; carrier gas: air.

Conclusions

Two novel large-pore sodium vanadium silicates, AM-15 and AM-17, with approximate framework compositions $Na_6Si_{14}V_4O_{39}$ and $Na_6Ca_2Si_{24}V_6O_{65}$, respectively, have been prepared hydrothermally. Spectroscopic techniques suggest that as-synthesised AM-15 contains both square pyramidal V^{IV} and tetrahedral V^{V}, whereas V^{IV} in AM-17 assumes octahedral coordination. The latter is an interesting catalyst for dehydrogenation reactions.

Experimental Section

Synthesis: The synthesis of AM-15 and AM-17 was carried out in Teflon-lined autoclaves under static hydrothermal conditions.

Synthesis of AM-15. An alkaline solution was made by mixing 5.08 g of sodium silicate solution (Na_2O 8 wt%, SiO_2 27 wt%, Merck), 8.27 g of H_2O and 0.55 g of NaOH (Merck). A second solution was made by mixing 7.61 g of H_2O with 1.02 g of $VOSO_4 \cdot 5H_2O$ (Merck). These two solutions were combined and stirred thoroughly.

Synthesis of AM-17. An alkaline solution was made by mixing 5.01 g of sodium silicate solution (Merck), 10.35 g of H_2O, and 0.10 g of $Ca(OH)_2$ (Aldrich). A second solution was made by mixing 5.53 g of H_2O with 1.00 g of $VOSO_4 \cdot 5H_2O$ (Merck). The AM-15 gel with a composition $6.7Na_2O{:}11.4SiO_2{:}V_2O_5{:}441H_2O$, and the AM-17 gel with a composition $3.3Na_2O{:}0.7CaO{:}11.3SiO_2{:}V_2O_5{:}441H_2O$, were autoclaved for three days at 230 °C. The crystalline powders were filtered off, washed and dried at room temperature.

Catalytic Tests: The catalytic reactions were carried out at atmospheric pressure in a fixed-bed stainless-steel reactor (height = 16 cm, internal diameter = 0.5 cm), which was charged with 50 mg

of catalyst. Prior to reaction, the catalyst was activated at 350 °C in a flow of argon (10 mL/min) for 2-propanol conversion or in a flow of air (2 mL/min) for ethanol oxidation. The reactant was fed using a syringe pump and mixed with the flowing gas before entering the reactor tube. The products were analysed by gas chromatography with a 30-metre long capillary column (DP1 fused silica phase) and an FID (flame ionisation detector).

Techniques: Powder XRD data were collected on an X'Pert MPD Philips diffractometer (CuK_α X-radiation) with a curved graphite monochromator, a fixed divergence slit (0.5°, irradiated length 10.00 mm), a progressive receiving slit (slit's height 0.2 mm) and a flat-plate sample holder, in a Bragg−Brentano para-focusing optics configuration. Intensity data were collected by the step counting method, step 0.02°, time 120 (AM-17) and 64 s (AM-15) in the 2θ range 3−40°. X-ray diffraction pattern auto-indexing was performed with DICVOL[30] from the resolved first 22 lines and checked with the Chekcell package.[31]

SEM images were recorded on a Hitachi S-4100 Field Emission Gun tungsten filament working with a voltage of 25000 V. Chemical composition was determined by energy dispersive analysis of X-rays (EDAX). TGA and DSC curves were measured with TGA-50 and DSC Shimadzu analysers. Samples were heated under air with a rate of 2 °C/min. Variable temperature in situ powder XRD was carried out using an Anton Parr high-temperature chamber with a 10 °C/min heating rate. Nitrogen adsorption measurements were performed using a Micromeritics ASAP 2010 V1.01 B automatic instrument at 77 K. Pore-size distributions were determined using the density functional theory (DFT) Plus Software for data files generated from the ASAP instrument. Adsorption of benzene, *m*-xylene and mesitylene was measured at 298 K using a gravimetric adsorption apparatus equipped with a CI electronic MK2−M5 microbalance and an Edwards Barocel pressure sensor. Before measurements, the samples were outgassed overnight at 573 K. EPR spectra were obtained at room temperature on a Bruker ESP 300E spectrometer, operating at 9.53 GHz. The g-values were obtained by reference to standard diphenylpicrylhydrazine (DPPH, $g = 2.0037$). FTIR spectra were recorded in absorbance mode on a Mattson Mod 7000 spectrophotometer, as KBr pellets, in the range 400−4000 cm^{-1}. The pellets were prepared by sample dispersion (0.2 mg) in a KBr matrix (150 mg) and pressed. The spectra were typically an average of 64 scans with 4 cm^{-1} resolution. DR UV/Vis was performed on a Jasco V-560 PC spectrometer using $BaSO_4$ as the reference material.

Acknowledgments

The authors thank, FCT, PRAXIS XXI, POCTI and FEDER (Portugal) for financial support.

[1] J. I. W. C. E. Arends, R. A. Sheldon, M. W. Wallau, V. Schuchardt, *Angew. Chem. Int. Ed. Engl.* **1997**, *36*, 1144.
[2] M. Zahedi-Niaki, S. J. M. Zaidi, S. Kaliaguine, *Appl. Catal. A: Gen.* **2000**, *196*, 9.
[3] P. R. H. Rao, A. A. Belhekar, S. G. Hedge, A. V. Ramaswamy, P. Ratnasamy, *J. Catal.* **1993**, *141*, 595.
[4] Y. Deng, C. Lettmann, W. F. Maier, *Appl. Catal. A: Gen.* **2001**, *214*, 31.
[5] P. R. H. Rao, R. Kumar, A. V. Ramaswamy, P. Ratnasamy, *Zeolites* **1993**, *13*, 663.
[6] T. Sen, V. Ramaswamy, S. Ganapathy, P. R. Rajamohanan, S. Sivasanker, *J. Phys. Chem.* **1996**, *100*, 3809.
[7] S. H. Chien, J. C. Ho, S. S. Mon, *Zeolites* **1997**, *18*, 182.
[8] Z. Luan, J. Xu, H. He, J. Klinowski, L. Kevan, *J. Phys. Chem.* **1996**, *100*, 19595.
[9] Z. Luan, D. Zhao, L. Kevan, *Microporous Mesoporous Mater.* **1998**, *20*, 93.
[10] G. Catana, R. R. Rao, B. M. Weckhuysen, P. Van Der Voort, E. F. Vansant, R. A. Schoonheydt, *J. Phys. Chem. B* **1998**, *102*, 8005.
[11] D. Wei, H. Wang, X. Feng, W. Chuch, P. Ravikovitch, M. Lyubovsky, C. Li, T. Takeguchi, G. L. Haller, *J. Phys. Chem. B* **1999**, *103*, 2113.
[12] Z. Luan, J. Y. Bae, L. Kevan, *Chem. Mater.* **2000**, *12*, 3202.
[13] L. X. Dai, K. Tabata, E. Suzuki, T. Tatsumi, *Chem. Mater.* **2001**, *13*, 208.
[14] M. Mathieu, P. Van Der Voort, B. M. Weckhuysen, R. R. Rao, G. Catana, R. A. Schoonheydt, E. F. Vansant, *J. Phys. Chem. B* **2001**, *105*, 3393.
[15] J. Rocha, P. Brandão, Z. Lin, M. W. Anderson, V. Alfredsson, O. Terasaki, *Angew. Chem. Int. Ed. Engl.* **1997**, *36*, 100.
[16] M. W. Anderson, O. Terasaki, T. Ohsuna, A. Philippou, S. P. Mackay, A. Ferreira, J. Rocha, S. Lidin, *Nature* **1994**, *367*, 347.
[17] X. Wang, L. Liu, A. J. Jacobson, *Angew. Chem. Int. Ed.* **2001**, *40*, 2174.
[18] H. T. Evans, *J. Am. Mineral. Sect. B* **1973**, *58*, 412.
[19] R. Rinaldi, J. J. Pluth, J. V. Smith, *Acta Crystallogr., Sect. B* **1975**, *31*, 1598.
[20] X. Wang, L. Liu, A. J. Jacobson, *J. Am. Chem. Soc.* **2002**, *124*, 7812.
[21] P. Brandão, H. Hanif, A. Philippou, A. Ferreira, P. Ribeiro-Claro, J. Rocha, M. W. Anderson, *Chem. Mater.* **2002**, *14*, 1053.
[22] P. Brandão, N. Hanif, A. Philippou, J. Rocha, M. W. Anderson,. *Proceedings of the 13th International Zeolite conference*, Montpellier, **2001**, 176.
[23] D. C. M. Dutoit, M. Schneider, P. Fabrizioli, A. Baiker, *Chem. Mater.* **1996**, *8*, 734.
[24] L. Frunza, P. Van Der Voort, E. F. Vansant, A. Schoonheydt, B. M. Weckhuysen, *Microporous Mesoporous Mater.* **2000**, *39*, 493.
[25] S. Higashimoto, M. Matsuoka, H. Yamashita, M. Anpo, O. Kitao, H. Hidaka, M. Che, E. Giamello, *J. Phys. Chem. B* **2000**, *104*, 10288.
[26] P. E. Hathaway, M. E. Davies, *J. Catal.* **1989**, *116*, 263.
[27] J. M. Miller, L. J. Lakshmi, *J. Catal.* **1999**, *184*, 68.
[28] L. Wang, R. Eguchi, H. Arai, T. Seiyama, *Chem. Lett.* **1986**, 1173.
[29] N. Iwasa, O. Yamamoto, R. Tamura, M. Nishikubo, N. Takezawa, *Catal. Lett.* **1999**, *62*, 179.
[30] A. Boultif, D. Louër, *J. Appl. Crystallogr.* **1991**, *21*, 987.
[31] J. Laugier, B. Bochu, *Programme D'affinement des Paramètres de Maille à Partir d'un Diagramme de Poudre*; Laboratoire des Matériaux et du Génie Physisque, École Nationale Supérieure de Physisque de Grenoble (INGP), Saint Martin d'Hères, France.

Received July 1, 2002
[I02357]